Event-Based Analysis of Rainfall Variability from Integrated GNSS-Derived Precipitable Water Vapor and Weather Radar Observations in Bangkok

Trakolkul, C.,[1] Charoenphon, C.,[2] Visessri, S.[3] and Satirapod, C.[2*]
[1]Faculty of Engineering and Architecture, Rajamangala University of Technology Suvarnabhumi, Thailand
E-mail: chokchai.t@rmutsb.ac.th, ORCID ID: https://orcid.org/0009-0006-2026-1488
[2]Mapping and Positioning from Space (MAPS) Research Center, Department of Survey Engineering, Faculty of Engineering, Chulalongkorn University, Thailand
E-mail: chaiyuth.c@chula.ac.th, ORCID ID: https://orcid.org/0000-0003-3887-8460
chalermchon.s@chula.ac.th* ORCID ID: https://orcid.org/0000-0003-2932-0334*
[3]Department of Water Resources Engineering, Faculty of Engineering, Chulalongkorn University, Thailand
Email: Supattra.vi@chula.ac.th, ORCID ID: https://orcid.org/0000-0003-1963-927X
**Corresponding Author*

DOI: https://doi.org/10.52939/ijg.v22i4.4939

Abstract
Short-term rainfall monitoring in tropical megacities remains challenging due to highly variable atmospheric conditions. This study evaluates the relationship between GNSS-derived precipitable water vapor (PWV) and rainfall occurrence, intensity, and duration in the Bangkok Metropolitan Region, Thailand. High-resolution GNSS data from five Continuously Operating Reference Stations (CORS) collected during 2019–2022 were processed using precise point positioning to estimate PWV from tropospheric delays. These PWV estimates were integrated with rainfall, relative humidity, and weather radar reflectivity data. Statistical analysis during the 2019–2022 rainy seasons indicates a weak linear relationship between PWV and 24-hour accumulated rainfall (Pearson $r = 0.15$, $p < 0.001$), but a stronger monotonic association (Spearman $\rho = 0.39$, $p < 0.001$), suggesting that rainfall response to atmospheric moisture is not strictly linear. Lag-correlation analysis shows that PWV typically precedes rainfall by approximately 8–9 hours. Detailed lag-based analysis was conducted at a representative GNSS station (DPT9) with minimal GNSS–gauge separation (≈4 km), reducing spatial representativeness uncertainty under convective rainfall conditions. Radar observations show spatial and temporal consistency between elevated PWV and organized precipitation systems during heavy and prolonged rainfall events. The integration of GNSS-derived PWV with meteorological and radar observations provides an observational basis for event-based rainfall assessment in urban environments.

Keywords: GNSS Meteorology, Precipitable Water Vapor, Rainfall Variability, Weather Radar, Precise Point Positioning, Urban Rainfall Assessment

1. Introduction

Accurate short-term rainfall monitoring in tropical urban regions remains a significant challenge because of the high spatial and temporal variability of atmospheric conditions. Bangkok, a densely populated metropolitan area, is particularly vulnerable to intense rainfall and urban flooding. Previous studies have shown that precipitable water vapor (PWV) derived from Global Navigation Satellite System (GNSS) observations provides valuable information for monitoring atmospheric moisture [1][2] and [3]. More recent research has highlighted the potential of GNSS-derived PWV to support rainfall analysis, particularly in tropical and monsoon-influenced regions [4][5] and [6]. In addition, GNSS-based water vapor analyses have been applied to characterize moisture variability associated with extreme precipitation events, such as typhoon-induced rainfall [7]. GNSS-derived PWV offers high temporal resolution, continuous monitoring, and broad spatial coverage at relatively low cost compared with traditional microwave radiometers [8]. Recent advances have extended GNSS-PWV applications toward spatial modeling. For instance, thin-plate spline interpolation has been applied to reconstruct regional water vapor fields from GNSS networks, improving representation of

spatial moisture variability [9]. Similarly, GNSS-derived PWV has been employed for monitoring atmospheric moisture conditions across different climatic regions [10]. Similar PWV variability and rainfall-related behavior have also been reported in other Asian monsoon environments. For instance, GPS-derived PWV variations and their relationship with rainfall have been examined during the Mei-yu season in Taiwan [11], while long-term PWV variability derived from GPS observations has also been analyzed over Taiwan [12]. These studies provide relevant regional context for interpreting PWV–rainfall relationships in monsoon-influenced environments. However, many existing studies primarily focus on rainfall occurrence, while rainfall characteristics such as intensity, duration, and spatial distribution remain less explored. In tropical convective environments, the relationship between atmospheric moisture and rainfall is often non-linear, making quantitative assessment of moisture–rainfall interactions challenging.

To address these gaps, this study integrates high-resolution GNSS-derived PWV from five Continuously Operating Reference Stations (CORS) in the Bangkok Metropolitan Region with surface meteorological observations and radar reflectivity data obtained from the Thai Meteorological Department. By combining these geospatial datasets, the study evaluates the relationship between atmospheric moisture and event-based rainfall variability. Previous research has shown that integration of GNSS-derived PWV with radar and meteorological observations can improve characterization of precipitation processes [13] and [14]. In tropical regions, the accuracy of PWV estimation depends on appropriate weighted mean temperature (*Tm*) models [15], and GNSS-derived PWV has shown associations with rainfall characteristics during flood events in Thailand [16]. More recently, advanced approaches for improving weighted mean temperature estimation, including deep learning-based models, have been explored to enhance GNSS meteorological applications [17]. Building on these developments, the present study investigates moisture–rainfall relationships in a tropical urban environment using an event-based analytical framework. While previous studies have demonstrated associations between GNSS-derived PWV and rainfall occurrence, fewer studies have examined how PWV variability relates to different rainfall event types and their temporal evolution in densely urbanized tropical regions. This study combines PWV observations from multiple CORS stations with radar reflectivity and surface meteorological data to examine rainfall variability at the event scale. Particular emphasis is placed on the temporal lead–lag relationship between PWV and rainfall and on the characterization of different rainfall patterns, including heavy rainfall, prolonged rainfall, and no-rain events. Rather than focusing on predictive modeling, the analysis emphasizes geospatial consistency across GNSS, radar, and rain gauge observations to better interpret moisture–precipitation coupling in monsoon-influenced urban environments. This framework provides an observational basis for understanding how atmospheric moisture conditions evolve prior to different rainfall regimes in tropical megacities.

2. Data and methods

2.1 Study Area and Datasets

This study focuses on the Bangkok Metropolitan Region (BMR), Thailand, which includes Bangkok and the surrounding provinces of Nonthaburi, Pathum Thani, Samut Prakan, Samut Sakhon, and Nakhon Pathom (Figure 1). The region is characterized by low-lying terrain and a tropical monsoon climate, with pronounced seasonal rainfall and frequent convective precipitation. Owing to its high population density and vulnerability to intense rainfall and urban flooding, the BMR provides an appropriate setting for investigating the relationship between atmospheric moisture and rainfall characteristics. Multiple datasets were used to support the integrated analysis of atmospheric moisture and precipitation. GNSS observation data were obtained from five Continuously Operating Reference Stations (CORS) distributed across the study area and processed to derive precipitable water vapor (PWV), representing column-integrated atmospheric moisture. The reliability and coordinate consistency of the Thai national GNSS CORS network have been previously assessed and validated [18], supporting its suitability for geodetic and atmospheric applications across Thailand. Meteorological observations, including rainfall, relative humidity, and wind information, were acquired from surface stations operated by the Thai Meteorological Department. In addition, weather radar data covering the study area were used to obtain radar reflectivity (dBZ), which describes the spatial structure and relative intensity of precipitation systems. Meteorological stations were selected based on proximity to the GNSS CORS sites to maintain spatial consistency in PWV–rainfall comparisons.

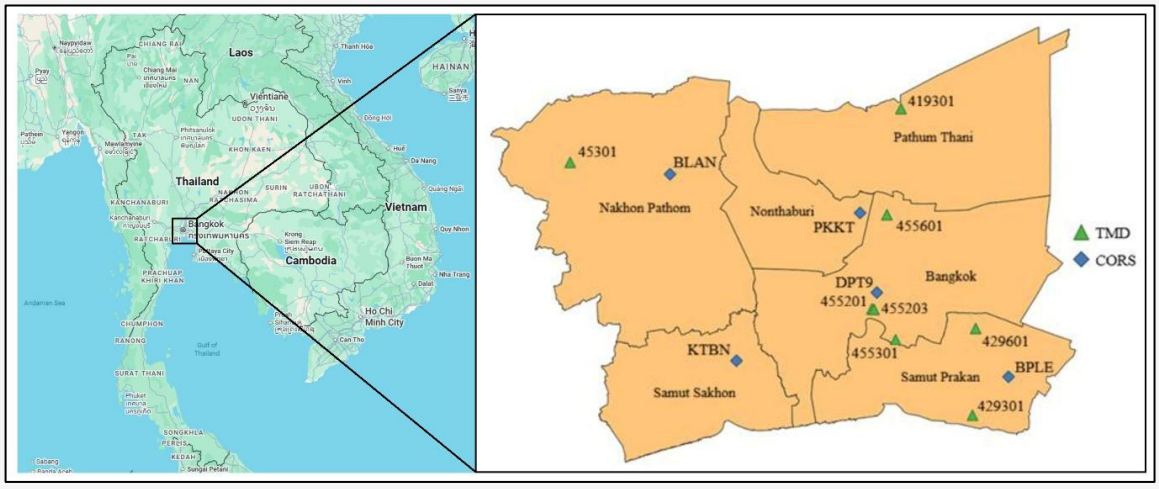

Figure 1: Spatial distribution of GNSS Continuously Operating Reference Stations (CORS) and Thai Meteorological Department (TMD) observation stations within the Bangkok Metropolitan Region, Thailand

Table 1: Distances between GNSS CORS stations and the nearest meteorological stations used for rainfall and atmospheric data analysis

GNSS Station	Latitude (˚)	Longitude (˚)	TMD Station	Latitude (˚)	Longitude (˚)	Distance (km)
BLAN	13.9881	100.1663	451301	14.0114	99.9699	21
PKKT	13.9125	100.5401	419301	14.1162	100.6206	24
			455601	13.9090	100.5930	6
DPT9	13.7568	100.5732	455201	13.7246	100.5633	4
			455203	13.7238	100.5677	6
			455301	13.6644	100.6099	11
BPLE	13.5920	100.8321	429601	13.6864	100.7675	13
			429301	13.5169	100.7613	11
KTBN	13.6234	100.2971	455201	13.7246	100.5633	31

2.2 GNSS-Based Retrieval of Precipitable Water Vapor

High-resolution atmospheric water vapor was estimated from GNSS observations using the Precise Point Positioning (PPP) technique. GNSS data in RINEX format were processed with GipsyX software using precise IGS orbit and clock products to estimate the zenith total delay (ZTD) at each station [19]. In this study, ZTD, ZHD, and ZWD are expressed in meters, whereas PWV is reported in millimeters as the equivalent height of liquid water in the atmospheric column. The estimated ZTD was decomposed into zenith hydrostatic delay (ZHD) and zenith wet delay (ZWD) following established GNSS meteorology methods [1] and [20]. ZWD is defined in Equation 1.

$$ZWD = ZTD - ZHD$$

Equation 1

The hydrostatic delay was modeled using the Saastamoinen model in Equation 2 [21], which has been widely applied in tropical environments [22]:

$$ZHD = \frac{0.0022768Ps}{1\text{-}0.00266\cos(2\phi)\text{-}0.00000028H}$$

Equation 2

Where Ps is the surface pressure (hPa), ϕ is station latitude, and H is the station height above mean sea level (m). The wet delay (ZWD), which reflects atmospheric moisture content, was estimated during PPP processing. Precipitable water vapor (PWV) was derived from ZWD using a temperature-dependent conversion factor as presented in Equations 3 and 4 [1]:

$$PWV = \prod \times ZWD$$

Equation 3

Where:

$$\Pi = \frac{10^6}{\rho_w R_v \left(\frac{k_3}{T_m} + k'2\right)}$$

Equation 4

and ρ_w is the density of liquid water (999.97 kg m^{-3}), R_v is the specific gas constant for water vapor (461.5 J kg^{-1} K^{-1}), k'_2 and k_3 are refractivity constants, taken as 22.1 K hPa^{-1} and 3.739x10^5 K^2 hPa^{-1}, respectively. T_m is the weighted mean atmospheric temperature. In this study, T_m was estimated using a locally calibrated empirical model developed for tropical conditions [23]:

$$T_m = 0.6066T_s + 113.2914 \quad \text{Equation 5}$$

Where T_s is surface air temperature (K).

PWV values were generated at hourly intervals, providing continuous monitoring of atmospheric moisture variability across the Bangkok Metropolitan Region. Previous validation studies in Thailand have evaluated GNSS-derived PWV against radiosonde observations and ERA5 reanalysis datasets [15] and [16], supporting the use of the PWV dataset in rainfall-related analysis.

2.3 Weather Radar Data Processing

The data processing workflow presents in Figure 2. Weather radar observations from the Samut Songkhram C-band dual-polarization radar operated by the Thai Meteorological Department were used to complement the GNSS-derived PWV dataset. The radar provides reflectivity measurements (dBZ) that describe the spatial structure and relative intensity of precipitation systems [24]. Raw radar data in Universal Format (UF) were converted to CfRadial NetCDF format using LROSE software tools (RadxConvert and HawkEye). The converted data were subsequently georeferenced to generate reflectivity fields covering the study area. Radar reflectivity was used to characterize the spatial distribution and organization of precipitation systems rather than to derive quantitative rainfall rates. Reflectivity values were interpreted according to standard dBZ intensity ranges (Table 2). Surface rainfall intensity was determined independently from rain gauge measurements and classified using gauge-based thresholds (Table 3). No Z–R relationship was applied in this study in order to avoid uncertainties associated with regional variability of Z–R parameters. Radar reflectivity and gauge-derived rainfall measurements therefore serve complementary roles: reflectivity describes spatial precipitation structure, while rain gauges provide quantitative surface rainfall intensity.

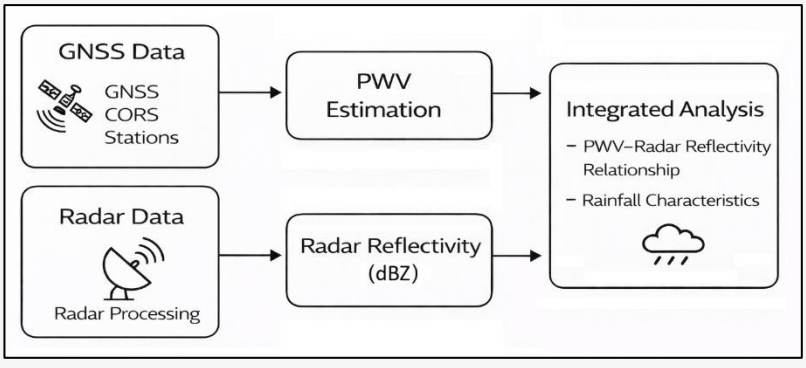

Figure 2: Workflow of data processing and integrated analysis. The workflow illustrates GNSS data processing for precipitable water vapor (PWV) estimation, weather radar data processing for reflectivity retrieval, and the integration of these datasets to analyze rainfall occurrence, intensity, and duration

Table 2: Radar reflectivity intensity ranges used for precipitation classification

Reflectivity (dBZ)	General precipitation description
< 0	No detectable precipitation
0 - 20	Very light precipitation
20 - 30	Light precipitation
30 - 40	Moderate precipitation
40 - 50	Heavy precipitation
50 - 55	Very heavy precipitation
> 55	Intense precipitation or possible hail

Table 3: Rainfall intensity categories based on rain gauge measurements

Rainfall Rate (mm h^{-1})	Intensity classification
0.1 – 5.0	Light
5.1 – 25.0	Moderate
25.1 – 50.0	Heavy
≥50.0	Very heavy

2.4 Integrated Data Analysis

An integrated analysis framework was applied to examine spatial and temporal relationships between atmospheric moisture and rainfall events. Hourly GNSS-derived PWV time series from all five CORS stations were combined with 15-minute radar reflectivity observations and surface meteorological measurements, including rainfall and relative humidity. GNSS station coordinates derived from PPP processing were used to ensure spatial alignment between PWV estimates, radar data, and meteorological observations. Meteorological stations were selected based on proximity to GNSS CORS sites to maintain spatial consistency in PWV–rainfall comparisons.

For detailed lead–lag and event-based rainfall coupling analysis, station DPT9 was selected as the primary site because it provides the smallest GNSS–rain gauge separation (approximately 4 km), thereby reducing spatial representativeness uncertainty under localized convective rainfall conditions. Radar-based event interpretation was also focused on DPT9 because the radar observations used in this study were obtained from a single radar dataset covering the study area, and DPT9 is the CORS station located closest to the corresponding rain gauge used in the analysis. This site therefore provides the most suitable basis for integrating GNSS-derived PWV, rain gauge observations, and radar reflectivity within a consistent event-scale framework. Event-based analysis was conducted to characterize different rainfall patterns, including heavy rainfall, prolonged rainfall, and no-rainfall events. Temporal variations in PWV were examined together with radar reflectivity structure and surface rainfall intensity to assess moisture–rainfall relationships at the event scale. This integrated approach emphasizes geospatial consistency across datasets and supports assessment of rainfall variability in a tropical urban environment. For lag-correlation analysis, the hourly PWV series and the 3-hourly rainfall series were compared using their original observation timestamps without temporal interpolation. Lag was evaluated by shifting the relative timing between the two datasets while preserving their native temporal resolution. This approach was adopted to avoid introducing additional uncertainty through resampling or interpolation of the rainfall observations.

3. Results

3.1 Relationship between Precipitable Water Vapor (PWV) and Rainfall

Rainfall data used in this analysis were obtained from meteorological stations located near the GNSS CORS sites to ensure spatial consistency in PWV–rainfall comparisons. Following previous studies [25], stations within 8 km of the corresponding CORS sites were considered. Station DPT9 was selected for detailed analysis because of its close proximity (approximately 4 km) to the corresponding rain gauge (Table 1). Although five CORS stations were available in the study area, lag-based statistical analysis was conducted at DPT9 to minimize spatial representativeness uncertainty associated with convective rainfall. Time series analysis of PWV and 24-hour accumulated rainfall during the 2019–2022 rainy seasons shows distinct temporal variability in rainfall and comparatively smoother variations in PWV (Figure 3). PWV ranged from 35.2 mm to 67.2 mm, with a standard deviation of ±4.7 mm. Daily rainfall ranged from 0.1 mm to 128.6 mm, with a mean of 15.4 mm and a standard deviation of ±20.3 mm. Periods of elevated PWV were frequently associated with higher daily rainfall accumulation.

Correlation analysis indicates a statistically significant but weak linear relationship between PWV and daily rainfall (Pearson $r = 0.15$). Spearman rank correlation analysis shows a moderate monotonic association ($\rho = 0.39$, $p < 0.001$, $n = 680$), indicating that higher PWV values are generally associated with increased rainfall magnitude, although the relationship is not strictly linear. Lag-correlation analysis was performed using hourly PWV observations and 3-hourly rainfall records at their original observation timestamps, without temporal interpolation. Correlation values increase when PWV leads rainfall. The maximum monotonic association (Spearman $\rho \approx 0.34$) occurs at a lag of −8 to −9 hours, where negative lag indicates PWV leading rainfall. As illustrated in Figure 4, correlation coefficients increase from near-zero lag toward negative lag values and reach a maximum at approximately −8 hours. Correlation decreases beyond this lead time and remains weaker at positive lags, where rainfall precedes PWV. This pattern supports the interpretation that PWV is more commonly elevated prior to rainfall events than after rainfall has occurred.

Seasonal analysis for 2020 further illustrates the lag and correlation patterns described above (Figure 5). Comparison between PWV at DPT9 and the network-mean PWV derived from the five CORS stations indicates that local moisture variability at the reference site generally occurs within broader regional atmospheric moisture fluctuations across the Bangkok Metropolitan Region. The close similarity between the two series reflects the strong regional coherence of atmospheric moisture conditions during the rainy season. While the network-mean PWV shows smoother temporal variability, PWV at DPT9 exhibits slightly stronger short-term fluctuations associated with rainfall events recorded at station 455201. The seasonal comparison in Figure 5 is consistent with the statistical results and indicates that the lag-based PWV–rainfall relationship identified at DPT9 is embedded within a broader regional moisture pattern. The similarity between the DPT9 and network-mean PWV series suggests that the reference site captures the regional moisture background reasonably well, while still preserving local event-scale variability relevant to rainfall coupling analysis.

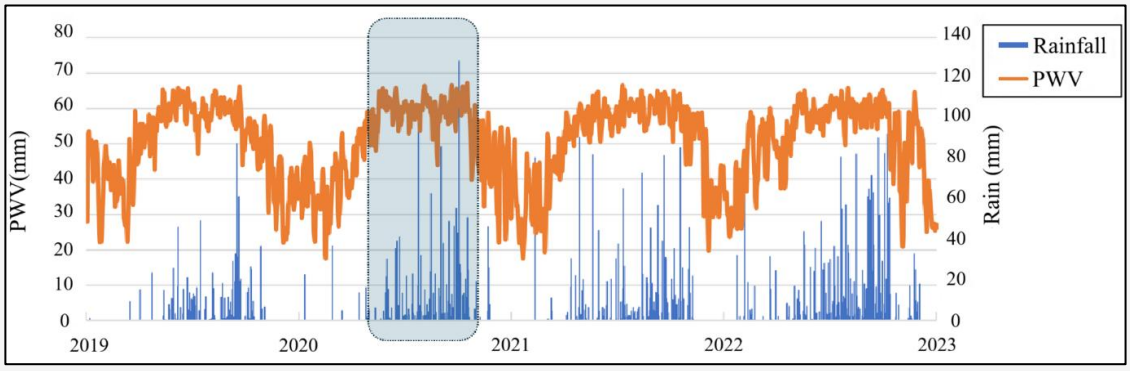

Figure 3: Time series of GNSS-derived precipitable water vapor (PWV) at station DPT9 (orange line) and 24-hour accumulated rainfall recorded at station 455201 (blue bars) during the rainy seasons from 2019 to 2022. PWV exhibits a clear seasonal pattern with relatively low variability, reaching higher values during the rainy season (May–October)

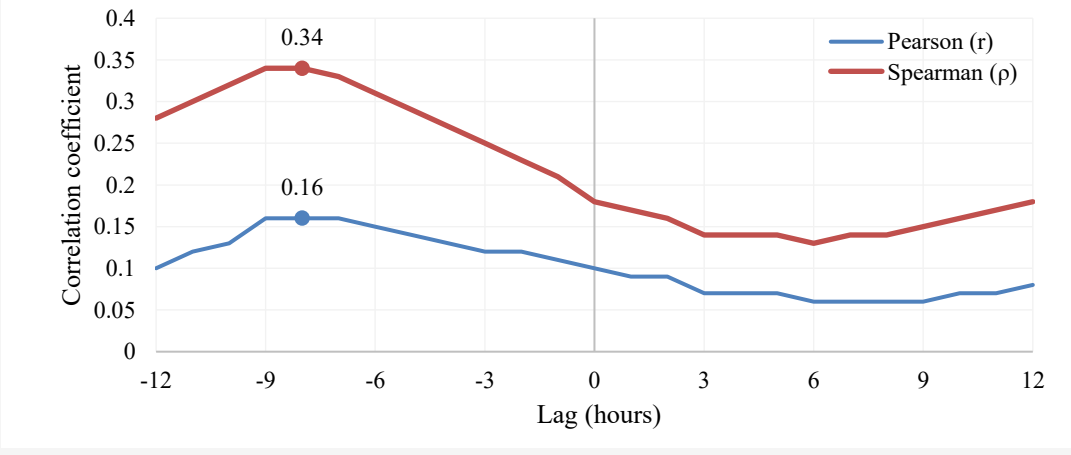

Figure 4: Lag correlation between hourly PWV and rainfall during the rainy season (2019–2022), shown for both negative and positive lag times. Negative lags indicate PWV leading rainfall, whereas positive lags indicate rainfall leading PWV. The maximum monotonic association occurs at approximately −8 to −9 hours (Spearman ρ = 0.34), indicating that PWV tends to increase several hours prior to rainfall

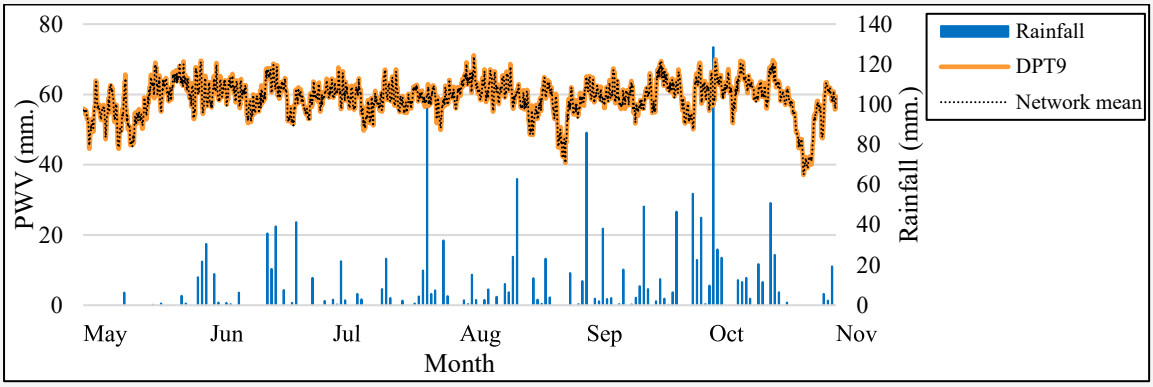

Figure 5: Comparison of GNSS-derived precipitable water vapor (PWV) at station DPT9 (orange line), network-mean PWV calculated from the five CORS stations (gray dashed line), and daily rainfall recorded at meteorological station 455201 (blue bars) during the 2020 rainy season (May–October). The close similarity between the DPT9 and network-mean PWV series indicates that local moisture variability at the reference site is embedded within a broader regional atmospheric moisture pattern

3.2 Relationship between PWV and Radar Reflectivity

The relationship between PWV and radar reflectivity was examined using data from GNSS station DPT9 and the nearby meteorological station 455201. This radar-focused analysis was conducted at DPT9 because it is the CORS station located closest to the rain gauge used for comparison and provides the smallest GNSS–rain gauge separation among the available stations. In addition, radar observations used in this study were obtained from a single radar dataset covering the study area, making DPT9 the most suitable location for consistent comparison between column-integrated PWV, point rainfall measurements, and radar reflectivity patterns. Radar reflectivity fields were spatially aligned with the GNSS station location to compare moisture variability with precipitation structure. Periods of elevated PWV frequently coincided with enhanced radar reflectivity during the rainy season. However, elevated PWV did not consistently correspond to measurable rainfall, particularly under conditions of high background moisture. This pattern indicates that moisture availability alone does not determine rainfall occurrence.

Rainfall events were classified into three types for comparison. Heavy rainfall events were defined as days with 24-hour accumulated rainfall exceeding 50 mm. Prolonged rainfall events were defined as rainfall persisting for more than 12 consecutive hours with cumulative accumulation exceeding 30 mm. No-rain events were defined as periods with 0 mm rainfall over 24 hours. These thresholds were applied consistently across the 2019–2022 rainy seasons to ensure reproducible classification. The cases presented in Figure 6 are illustrative examples selected from a larger set of events identified using the classification criteria described above. They are used to demonstrate typical temporal and spatial characteristics of each event type rather than to represent a statistical summary of the full event sample. Heavy rainfall events, such as 24 July 2020, were characterized by elevated PWV and localized high reflectivity, indicating intense but short-duration precipitation (Figure 6(a)–(b)). Prolonged rainfall events (16–17 October 2020) showed sustained high PWV accompanied by broader spatial reflectivity coverage over extended periods (Figure 6(e)–(f)). In contrast, no-rain events exhibited relatively stable PWV and weak reflectivity despite moderate atmospheric moisture (Figure 6(c)–(d)). Relative humidity is included in Figure 6 as supplementary information on near-surface moisture conditions during the selected events. Although it was not used as a primary classification variable in this study, it provides additional context for interpreting moisture conditions associated with rainfall development. Radar reflectivity in Figure 6 is used for qualitative interpretation of precipitation structure and relative intensity rather than for quantitative statistical comparison across all events.

The illustrative cases in Figure 6 suggest that prolonged rainfall events may be associated with broader reflectivity coverage, whereas heavy rainfall events tend to show more localized but higher-intensity reflectivity. These differences are consistent with the interpretation that rainfall intensity and duration are influenced by both moisture availability and storm organization.

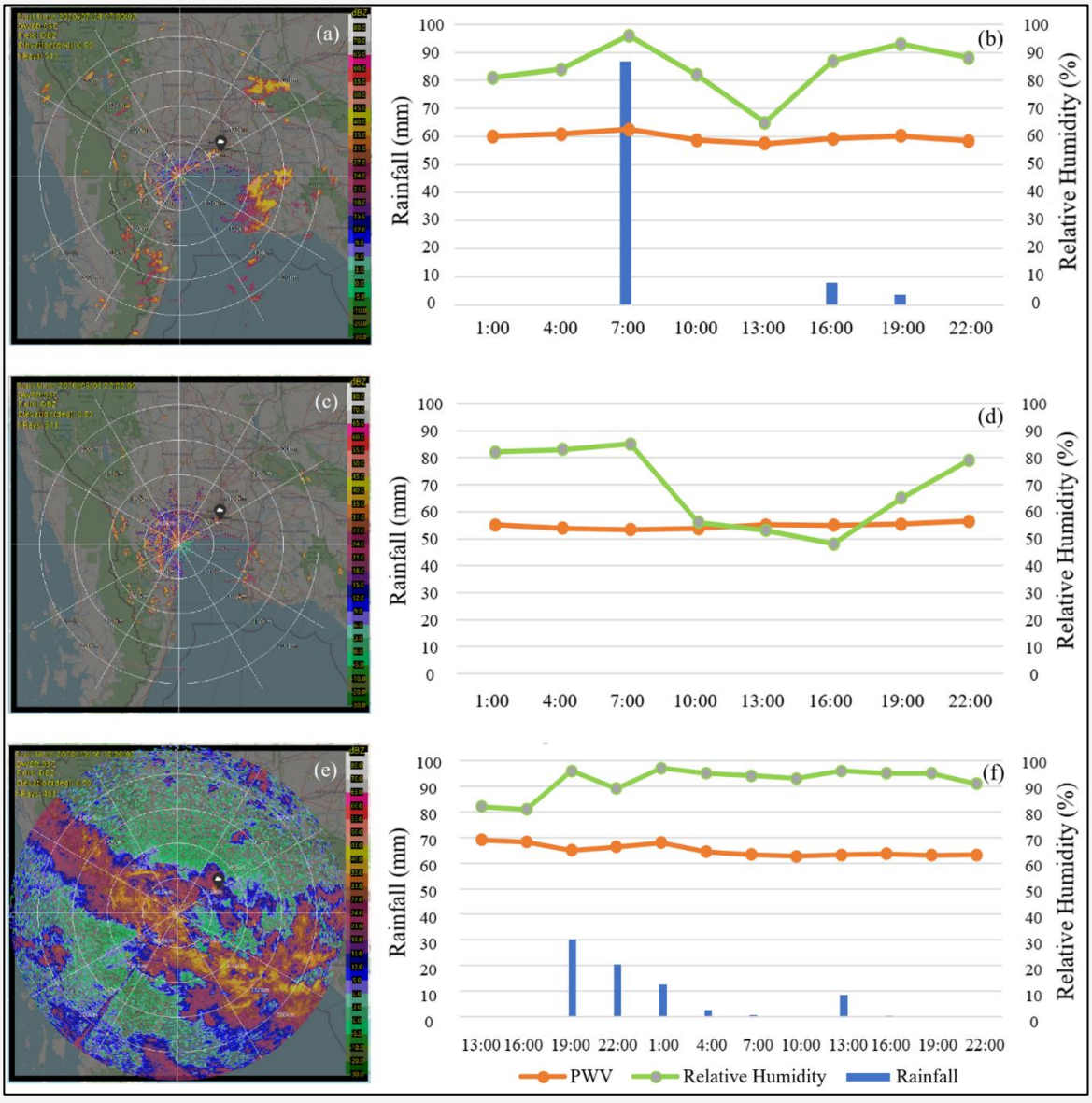

Figure 6: Radar reflectivity (dBZ) and GNSS-derived precipitable water vapor (PWV) during different rainfall event types at station DPT9. Panels (a, b) show a heavy rainfall event on 24 July 2020, panels (c, d) a no-rainfall event on 5 May 2020, and panels (e, f) a prolonged rainfall event during 16–17 October 2020. Left panels illustrate radar reflectivity, while right panels show the corresponding time series of PWV, rainfall, and relative humidity

4. Discussion

4.1 PWV as an Indicator of Rainfall

The results indicate that GNSS-derived precipitable water vapor (PWV) reflects atmospheric moisture conditions associated with rainfall events. During heavy and prolonged rainfall cases, elevated PWV values were commonly observed prior to or concurrent with recorded precipitation. In contrast, the no-rainfall case indicates that increased PWV alone does not necessarily result in rainfall, particularly under conditions of high background moisture. The difference between the Pearson ($r = 0.15$) and Spearman ($\rho = 0.39$) coefficients suggests that the PWV–rainfall relationship is not strictly linear. While PWV does not exhibit strong linear dependence on rainfall magnitude, the moderate monotonic association indicates that higher moisture levels are generally associated with increased rainfall occurrence or intensity. Lag-correlation results further show that the maximum association occurs when PWV leads rainfall by approximately 8–9 hours, supporting the interpretation that PWV

reflects pre-rainfall moisture accumulation rather than the rainfall process itself.

Although the lag-correlation coefficients remain modest, the pattern observed in Figure 4 is still meteorologically meaningful because it indicates that PWV tends to increase prior to rainfall rather than after rainfall has occurred. This behavior is consistent with the interpretation of PWV as an indicator of atmospheric moisture accumulation rather than a direct predictor of rainfall amount. The reported lead time should be interpreted in relation to the adopted temporal sampling structure, and further evaluation of alternative resampling strategies would be useful in future studies. Comparable PWV variability and rainfall-related behavior have also been reported in other Asian monsoon environments, including Taiwan [11] and [12], providing broader regional context for the lead–lag relationship identified in this study. More generally, similar lead–lag behavior has also been reported in GNSS-based studies conducted in other climatic regions [9] and [10], suggesting that such temporal moisture build-up patterns are not limited to the Bangkok Metropolitan Region. Overall, PWV should be interpreted as an indicator of favorable moisture conditions rather than a deterministic predictor of rainfall magnitude.

4.2 Integration of PWV, Radar, and Meteorological Data

The integration of GNSS-derived PWV with radar reflectivity and surface meteorological observations provides complementary information on rainfall variability. PWV represents column-integrated atmospheric moisture, whereas radar reflectivity describes the spatial structure and relative intensity of precipitation systems. Event-based analysis shows that heavy rainfall events are associated with elevated PWV and localized high reflectivity, while prolonged rainfall events exhibit sustained high PWV and broader reflectivity coverage. These spatial differences indicate that rainfall intensity and duration are influenced by both moisture availability and storm organization. The combined use of GNSS and radar observations supports a more consistent interpretation of moisture–precipitation relationships at the event scale. Similar integration strategies have been applied in GNSS meteorology studies in other regions [6] and [13], indicating that the approach is transferable beyond the present study area.

4.3 Implications for Rainfall Monitoring

The observed lead–lag behavior and event-based patterns suggest that GNSS-derived PWV can contribute to short-term rainfall monitoring when interpreted together with radar and surface meteorological data. Elevated PWV prior to rainfall events indicates moisture accumulation, while radar reflectivity provides spatial context for precipitation development. Given the weak linear but moderate monotonic association identified in this study, PWV should be regarded as a probabilistic indicator of moisture conditions rather than a direct predictor of rainfall amount. A limitation of this study is that detailed lag-based results are presented for one representative station. Although PWV was retrieved for multiple CORS sites, event-scale rainfall coupling was examined at station DPT9 to reduce spatial mismatch between column-integrated PWV and point rainfall measurements under convective conditions. Extending the lead–lag analysis to additional stations would provide further assessment of spatial consistency across the Bangkok Metropolitan Region. From an applied perspective, integrating PWV with radar observations provides complementary information for assessing rainfall variability in urban environments. Future work may incorporate additional atmospheric variables to further evaluate the consistency of the observed moisture–rainfall relationships.

5. Conclusions and Future Work

This study shows that GNSS-derived precipitable water vapor (PWV) reflects variations in atmospheric moisture and exhibits a weak linear ($r = 0.15$) but moderate monotonic (Spearman $\rho = 0.39$, $p < 0.001$) association with 24-hour accumulated rainfall during the rainy season. The observed lead–lag relationship, with PWV preceding rainfall by approximately 8–9 hours, indicates that PWV represents moisture accumulation prior to rainfall rather than direct rainfall occurrence. Integration of radar reflectivity with PWV and surface meteorological observations provides complementary information on rainfall variability, particularly in distinguishing heavy and prolonged rainfall events. The results suggest that combined geospatial analysis of GNSS and radar data can support event-based rainfall assessment in urban environments. Although PWV observations were available from five GNSS CORS stations, detailed rainfall coupling analysis was conducted at a representative site to reduce spatial mismatch between column-integrated PWV and point rainfall measurements. Radar-based event interpretation in this study was also based on a single radar dataset covering the study area, which reinforced the use of one spatially consistent reference site for integrated analysis. Future work may extend the analysis to additional GNSS stations to evaluate spatial consistency across the Bangkok Metropolitan Region. Increasing the temporal resolution of rainfall

measurements and improving radar data coverage may further refine PWV–rainfall analysis. Incorporating additional atmospheric variables, such as wind information, could also support more detailed assessment of moisture transport and rainfall timing.

Acknowledgments

The authors acknowledge the National CORS Data Center (NCDC) for providing GNSS observation data. This research was supported by the Mapping and Positioning from Space (MAPS) Research Center.

References

[1] Bevis, M., Businger, S., Herring, T. A., Rocken, C., Anthes, R. A. and Ware, R. H., (1992). GPS Meteorology: Remote Sensing of Atmospheric Water Vapor using the Global Positioning System. *Journal of Geophysical Research: Atmospheres*, Vol. 97(14), 15787–15801.

[2] Bevis, M., Businger, S., Chiswell, S., Herring, T. A., Anthes, R. A., Rocken, C. and Ware, R. H., (1994). GPS Meteorology: Mapping Zenith Wet Delays onto Precipitable Water. *Journal of Applied Meteorology*, Vol. 33(3), 379–386.

[3] Rocken, C., Hove, T. V., Johnson, J., Solheim, F., Ware, R., Bevis, M., Chiswell, S. and Businger, S., (1995). GPS/STORM-GPS Sensing of Atmospheric Water Vapor for Meteorology. *Journal of Atmospheric and Oceanic Technology*, Vol. 12(3), 468–478.

[4] Jin, S. and Luo, O.F., (2009). Variability and Climatology of PWV from Global 13-year GPS Observations. *IEEE Transactions on Geoscience and Remote Sensing*, Vol. 47(7), 1918–1924. https://doi.org/10.1109/TGRS.2008.2010401.

[5] Yin, W., Zhou, C., Tian, Y., Qiu, H., Zhang, W., Chen, H., Liu, P., Zhao, Q., Kong, J. and Yao, Y., (2025). Accurate Rainfall Prediction using GNSS PWV Based on Pre-Trained Transformer Model. *Remote Sensing*, Vol. 17(12). https://doi.org/10.3390/rs17122023.

[6] Gong, Y., Liu, Z., Chan, P. W. and Hon, K. K., (2023). Assimilating GNSS PWV and Radiosonde Meteorological Profiles to Improve PWV and Rainfall Forecasting Performance from the WRF Model over South China. *Atmospheric Research*, Vol. 286. https://doi.org/10.1016/j.atmosres.2023.106677.

[7] Zhou, L., Liang, H., Cao, Y., Fan, L., Shi, C. and Satirapod, C., (2025). Characteristic Analysis of Water Vapor Variation using GNSS Tomography during the 2023 Typhoon-Induced Rainstorm in the Jingjinji Area, China. *Atmospheric Research*, Vol. 328. https://doi.org/10.1016/j.atmosres.2025.108442.

[8] Li, L., Zhang, K., Wu, S., Li, H., Wang, X., Hu, A., Li, W., Fu, E., Zhang, M. and Shen, Z., (2022). An Improved Method for Rainfall Forecast Based on GNSS-PWV. *Remote Sensing*, Vol. 14(17). https://doi.org/10.3390/rs14174280.

[9] Ansari, K., Walo, J., Wezka, K., Marjanska, D. and Jamjareegulgarn, P., (2025). Thin-plate Spline Interpolation Spatial Modelling of GNSS Retrieved Water Vapor Over Northeast Japan. *International Journal of Climatology*, Vol. 45(1), 1–14. https://doi.org/10.1002/joc.8704.

[10] Ansari, K., Althuwaynee, O. F. and Corumluoglu, O., (2016). Monitoring and Prediction of Precipitable Water Vapor using GPS Data in Turkey. *Journal of Applied Geodesy*, Vol. 10(4), 233–245. https://doi.org/10.1515/jag-2016-0037.

[11] Lien, T. Y., Yeh, T. K., Hong, J. S. and Hsiao, T. Y., (2022). Variations in GPS Precipitable Water Vapor and Rainfall during the 2006–2019 Mei-yu Season in Taiwan. *Advances in Space Research,* Vol. 70(5), 1375–1387. https://doi.org/10.1016/j.asr.2022.05.065.

[12] Pang, S. C., Yeh, T. K., Hong, J. S. and Chen, C. H., (2021). Variability and Climatology of Precipitable Water Vapor from 12-year GPS Observations in Taiwan. *Advances in Space Research,* Vol. 67(8), 2333–2346. https://doi.org/10.1016/j.asr.2021.01.021.

[13] Ma, Z., Guo, G., Cai, M., Chen, X., Li, W. and Zhang, L., (2022). A Combined Linear–Nonlinear Short-Term Rainfall Forecast Method using GNSS-derived PWV. *Atmosphere*, Vol. 13(9). https://doi.org/10.3390/atmos13091381.

[14] Wu, F., Zhang, K., Zhao, J., Jin, Y. and Li, D., (2023). Linear and Nonlinear GNSS PWV Features for Heavy Rainfall Forecasting. *Advances in Space Research*, Vol. 72(6). https://doi.org/10.1016/j.asr.2023.05.028.

[15] Charoenphon, C., Trakolkul, C. and Satirapod, C., (2022). Performance Assessment of Weighted Mean Temperature Models Derived from AIRS and ERA5 Reanalysis for Calculating GPS Precipitable Water Vapor in the Thailand Region. *Acta Geodaetica et Geophysica*, Vol. 57, 661–675. https://doi.org/10.1007/s40328-022-00397-1.

[16] Trakolkul, C., Charoenphon, C. and Satirapod, C., (2024). Investigating the Relationship between Precipitable Water Vapor and Rainfall Data During Flood Events: A GNSS-based Study in Thailand. *International Journal of Geoinformatics*, Vol. 20(11), 1–10. https://doi.org/10.52939/ijg.v20i11.3677.

[17] Charoenphon, C., Panboonyuen, T., Trakolkul, C., Zhang, B. and Satirapod, C., (2025). Investigating the use of Deep Learning-Derived Weighted Mean Temperature for GPS-PWVs Estimation. *Journal of Spatial Science*, Vol. 70(3), 519–540. https://doi.org/10.1080/14498596.2025.2506695.

[18] Kriengkraiwasin, S., Charoenphon, C., Butwong, K., Kovitpongkajorn, V., Yomwan, P., Thongtan, T. and Satirapod, C., (2022). Unification of GNSS CORS Coordinates in Thailand. *Survey Review*, Vol. 54(387), 534–542. https://doi.org/10.1080/00396265.2021.1987002.

[19] Kouba, J. and Héroux, P., (2001). Precise Point Positioning using IGS Orbit and Clock Products. *GPS Solutions*, Vol. 5(2), 12–28.

[20] Davis, J. L., Herring, T. A. and Shapiro, I. I., (1991). Effects of Atmospheric Modeling Errors on Determinations of Baseline Vectors from Very Long Baseline Interferometry. *Journal of Geophysical Research: Solid Earth*, Vol. 96(1), 643–650. https://doi.org/10.1029/90JB01503.

[21] Saastamoinen, J., (1972). Contributions to the theory of atmospheric refraction. *Bulletin Géodésique*, Vol. 105(1), 279–298. https://doi.org/10.1007/BF02521844.

[22] Satirapod, C. and Chalermwattanachai, P., (2005). Impact of Different Tropospheric Models on GPS Baseline Accuracy: Case Study in Thailand. *Journal of Global Positioning Systems*, Vol. 4, 36–40. https://doi.org/10.5081/jgps.4.1.36.

[23] Suwantong, R., Srestasathiern, P., Satirapod, C., Chuang, S. and Kitpracha, C., (2017). Mean Atmospheric Temperature Model Estimation for GNSS Meteorology using AIRS and AMSU Data. *Engineering and Applied Science Research*, Vol. 44(1), 46–52.

[24] Doviak, R. J. and Zrnić, D. S., (1993). *Doppler Radar and Weather Observations*. Academic Press, San Diego, CA.

[25] Trakolkul, C. and Satirapod, C., (2021). Variations of Precipitable Water Vapor using GNSS CORS in Thailand. *Survey Review*, Vol. 53(376), 90–96. https://doi.org/10.1080/00396265.2020.1713611.